

FATIGUE CRACK GROWTH IN ELASTIC-PLASTIC MATERIALS UNDER COMBINED BENDING WITH TORSION

E. MACHA, D. ROZUMEK & R. PAWLICZEK

Department of Mechanics and Machine Design, Technical University of Opole, Opole, Poland.

ABSTRACT

The paper presents the results of tests on fatigue crack growth under proportional bending with torsion in the low-alloy 18G2A steel and AlCuMg1 aluminium alloy. Specimens with square sections and a stress concentrator in the form of an external one-sided sharp notch were used. The tests were performed under stress ratios $R = -1, -0.5$ and 0 . The test results are described by the ΔJ integral range and compared with the ΔK stress intensity factor range. It has been found that there is a good agreement between the test results and the model of crack growth rate, which includes the ΔJ integral range.

1 INTRODUCTION

Many failures are caused by crack growths in mixed modes of loading. In their paper, Qian and Fatemi [1] present a review of different criteria and quantities proposed in literature for the prediction of crack growth rate in mixed modes I, II and III. Yates [2], proposed a model for mixed mode (I + III) of fatigue crack growth equivalent to mode I. Specimens bent in three points were tested, and the crack position was initiated at a certain angle β to the bending plane. Thus, a combination of bending with torsion was obtained. It was found that the crack growth beginning in mode I was dependent on the orientation (direction) and crack opening displacement in the specimen tested. The presented model was proposed by Yates and Miller [3] for circumferential cracks. The author Kimachi et al. [4] tested the fatigue crack growth in the elastic-plastic material under tension with torsion. The test results were described with the J-integral, using a simple method (force versus deflection) and the finite element method. It was found [4] that the J-integral was the most appropriate fracture mechanics parameter for modes I and III in elastic-plastic materials. A good correlation between the above mentioned methods was obtained.

The aim of this paper is to describe mixed mode I and III crack growth with the ΔJ integral range and verify the proposed mathematical formula using as an example the test results for 18G2A construction steel and AlCuMg1 aluminium alloy.

2 EXPERIMENTS

Flat specimens made of a low-alloy higher-strength 18G2A steel and AlCuMg1 aluminium alloy were tested. The specimens were cut from a drawn rod, 16 mm in diameter and their dimensions were: length $l = 90$ mm, height $b = 10$ mm, thickness $g = 8$ mm (see Fig. 1).

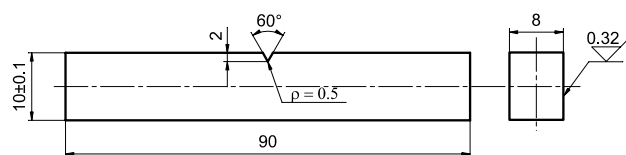


Figure 1: Specimen for tests of fatigue crack extension.

The specimens had an external unilateral notch, 2 mm deep and with the rounding radius $\rho = 0.5$ mm. The tests were performed for the following stress ratios: $R = -1, -0.5$ and 0 . The notches were cut with a cutter and their surfaces were polished after grinding. Chemical composition and some mechanical properties of the tested materials are given in Tables 1 to 4.

Table 1: Chemical composition of 18G2A steel.

C – 0.2%	Mn – 1.49%	Si – 0.33%	P – 0.023%	Fe Balance
S – 0.024%	Cr – 0.01%	Ni – 0.01%	Cu – 0.035%	

Table 2: Material properties of 18G2A steel.

σ_{YS} (MPa)	σ_{TS} (MPa)	E (GPa)	ν
357	535	210	0.3

Table 3: Chemical composition of AlCuMg1 aluminium alloy.

Cu – 4.15%	Mn – 0.65%	Zn – 0.50%	Mg – 0.69%	Al Balance
Fe – 0.70%	Cr – 0.10%	Si – 0.45%	Ti – 0.20%	

Table 4: Material properties of AlCuMg1 aluminium alloy.

σ_{YS} (MPa)	σ_{TS} (MPa)	E (GPa)	ν
395	545	72	0.32

Unilaterally restrained specimens were subjected to cyclic bending and torsion with a constant amplitude of moment $M_a = 17.19$ N·m (18G2A steel) and $M_a = 7.92$ N·m (AlCuMg1 aluminium alloy). The critical value of the integral for 18G2A steel is $J_{Ic} = 0.331$ MPa·m and AlCuMg1 aluminium alloy is $J_{Ic} = 0.026$ MPa·m [5]. Coefficients of the cyclic strain curve under tension-compression in the Ramberg-Osgood equation for 18G2A steel are the following (Macha and Rozumek [6]): the cyclic strength coefficient $K' = 869$ MPa, the cyclic strain hardening exponent $n' = 0.287$ and for AlCuMg1 aluminium alloy are $K' = 1779$ MPa, $n' = 0.234$. Crack development was observed on the specimen surface using the optical method. The fatigue crack increments were measured with a digital micrometer located in a portable microscope with magnification of 25 times and a sensitivity of 0.01 mm. At the same time, the number of loading cycles N was written down. The tests were performed under controlled loading from the threshold value to the specimen failure. The tests were performed on a fatigue test stand MZGS-100 (Achtelik [7], Fig. 2a) enabling realization of cyclically variable and static (mean) loading. Bending with torsion were tested for the ratio of torsional and bending moments $M_T(t)/M_B(t) = \text{tg}\alpha = \sqrt{3}$ (Fig. 2b) and loading frequency 29 Hz. The total moment $M(t) = 2M_B(t)$ was generated by force on the arm 0.2 m in length. The specimen (1) was fixed in holders (2) and (4). Loading was obtained as a result of the lever (5) motion in the vertical plane, generated by inertial force of the unbalanced mass (8) on the rotating disk (7) mounted on flat springs (9). The spring servo-motor (11), mounted on the base (3), enabled giving the mean loading by suitable spring (12) deflection. Mixed modes I and III were obtained by rotation of the head (2) (Fig. 2a) by angle $\alpha = 60^\circ$ (see Fig. 2b). When $\alpha = 0^\circ$, we have pure bending, for $\alpha = 90^\circ$ we obtain pure torsion. In the case of mixed mode I and III, the

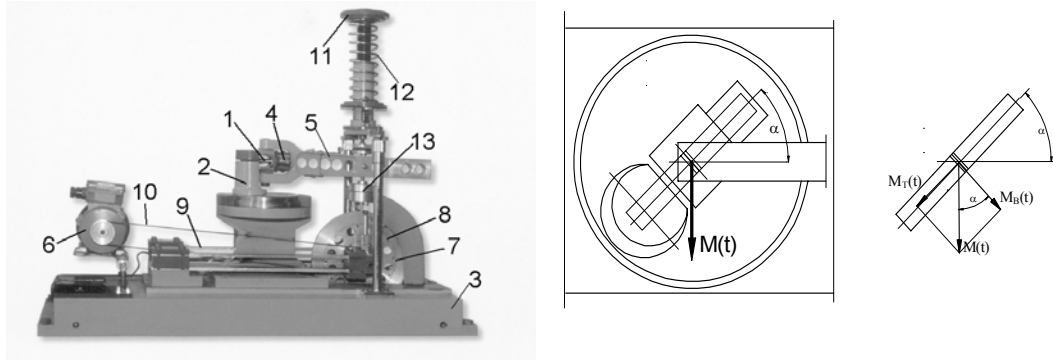


Figure 2: a) Fatigue test stand MZGS-100 and b) loading of the specimen.

range of the equivalent integral ΔJ_{eq} was assumed, according to Kimachi et al. [4], as the sum of ranges of integrals ΔJ_I and ΔJ_{III}

$$\Delta J_{eq} = \Delta J_I + \Delta J_{III} \quad (1)$$

The range of the equivalent stress intensity factor ΔK_{eq} under mixed mode I and III reduced to mode I can be written as

$$\Delta K_{eq} = \sqrt{(\Delta K_I^2 \sin^2 \alpha + 2.6 \Delta K_{III}^2 \cos^2 \alpha)} \quad (2)$$

using the Tresca yield criterion and the Yates relation [2].

The ranges of stress intensity factors ΔK_I for mode I and ΔK_{III} for mode III are the following:

$$\Delta K_I = \Delta \sigma \sqrt{\pi a} \sin^2 \alpha Y_1(a/w), \quad (3)$$

$$\Delta K_{III} = \Delta \tau \sqrt{\pi a} \sin \alpha \cos \alpha Y_3(a/w). \quad (4)$$

J-integrals were calculated with the finite element method (FEM), using the program franc2d (Rozumek [8]). The cyclic strain curve based on the nonlinear material model was introduced into the program franc2d. The introduced curve was the basis for calculations of stresses, strains and J-integrals. The calculations were performed for two-dimensional geometrical models of notched specimens. Fig. 3 shows the division of the notch region into finite elements. In the model six-nodal triangular elements were applied. For calculations, the same loading values as those used in

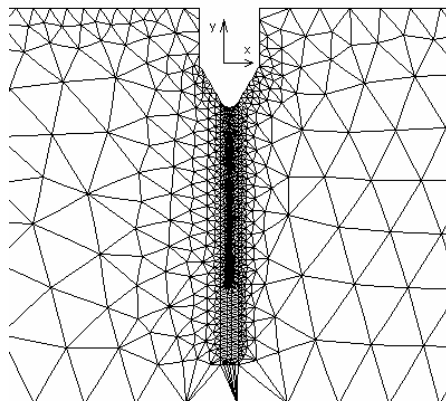


Figure 3: Division of the notch region into finite elements in the program franc2d.

experiments were assumed. In the linearly-elastic range, the ΔJ_{eq} integral ranges calculated with the equivalent stress intensity factor range ΔK_{eq} were compared with the results obtained from FEM. The relative error was below 5%. The experimental results for II and III range of crack growth rate were described with the following model (Rozumek [8])

$$\frac{da}{dN} = B \left(\frac{\Delta J}{J_0} \right)^n \sqrt{[(1-R)^2 J_{Ic} - \Delta J]} \quad (5)$$

where J_{Ic} – critical value of the J-integral, $\Delta J = J_{max} - J_{min}$, $J_0 = 1 \text{ MPa}\cdot\text{m}$ – unit value of the J-integral, B and n – coefficients were determined experimentally.

The test results were shown as graphs of the crack growth rate da/dN versus the ΔJ integral range. ΔJ was compared with the stress intensity factor range ΔK .

3 THE TEST RESULTS AND THEIR ANALYSIS

In Figs. 4a and 4b for modes I + III (graphs 1, 2, 3) it can be seen that the change of the stress ratio R from -1 to 0 is accompanied by an increase in the fatigue crack growth rate. Based on Figs. 4a and 4b, the fatigue crack growth rates in the tested materials were compared. From the graphs it results that for the stress ratio $R = -1$ the crack growth rates are similar. Moreover, it has been observed that influence of the loading mean value on the crack growth rate in the aluminium alloy AlCuMg1 is higher than in 18G2A steel despite the fact that the moment amplitude, M_a for the aluminium alloy is two times less. For example (Figs. 4a and 4b), while changing the value of the stress ratio from $R = -1$ to $R = 0$, a six fold increase in fatigue crack growth rate in 18G2A steel has been noticed, and in the aluminium alloy AlCuMg1 the fatigue crack growth rate was bigger by eleven times at the integral range corresponding to the beginning of the second crack range $\Delta J = 1 \cdot 10^{-2} \text{ MPa}\cdot\text{m}$ (18G2A steel) and $\Delta J = 4 \cdot 10^{-3} \text{ MPa}\cdot\text{m}$ (AlCuMg1 aluminium alloy).

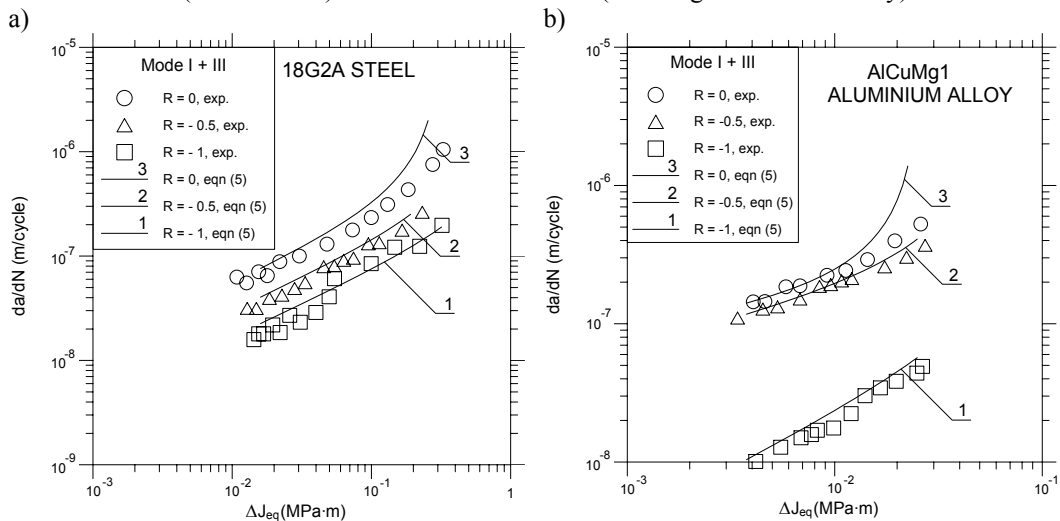


Figure 4: A comparison of the experimental results with calculated ones a) 18G2A, b) AlCuMg1.

It has also been found that ΔJ integral ranges are higher for 18G2A steel compared with AlCuMg1 aluminium alloy, which is due to different chemical composition of these materials and their different longitudinal moduli of elasticity E . The coefficients B and n occurring in eqn (5) were calculated with the least square method. The averaged values of these coefficients are for 18G2A steel $B = 3.5 \cdot 10^{-7} \text{ MPa}\cdot\text{m}^2 / \text{cycle}$ and $n = 0.62$ and for AlCuMg1 aluminium alloy $B = 0.9 \cdot 10^{-7} \text{ MPa}\cdot\text{m}^2 / \text{cycle}$ and $n = 0.40$ (the relative error of coefficient B for aluminium alloy is about 30% for $R = 0$). This implies that B and n are not material constants but they depend on other factors, such as the type of loading or mean value. The test results for cyclic bending with torsion include a relative error not exceeding 20% at the significance level $\alpha = 0.05$ for the correlation coefficients, r from 0.98 to 0.99 and the stress ratios, R from -1 to 0 . The coefficients of multiple correlation in all the cases take high values, so there is a significant correlation between the experimental results with the assumed model (5).

Calculating ΔJ_{eq} integral range for mixed mode I + III, we can find that there is a functional relation between the loading range, the elastic-plastic strain range, the crack opening and the crack length. Large values of correlation coefficients show that all these factors were approximately included. Above a certain value of ΔJ_{eq} integral range, the crack growth rate increases rapidly without further increase of loading. Such behaviour is connected with an unstable crack growth rate in the final stage of specimen life. In this period the stress drop can be observed as plasticization increases. Application of the ΔJ parameter is reasonable in the case of elastic-plastic materials and those with a distinct yield point. In order to prove applicability of ΔJ , the authors

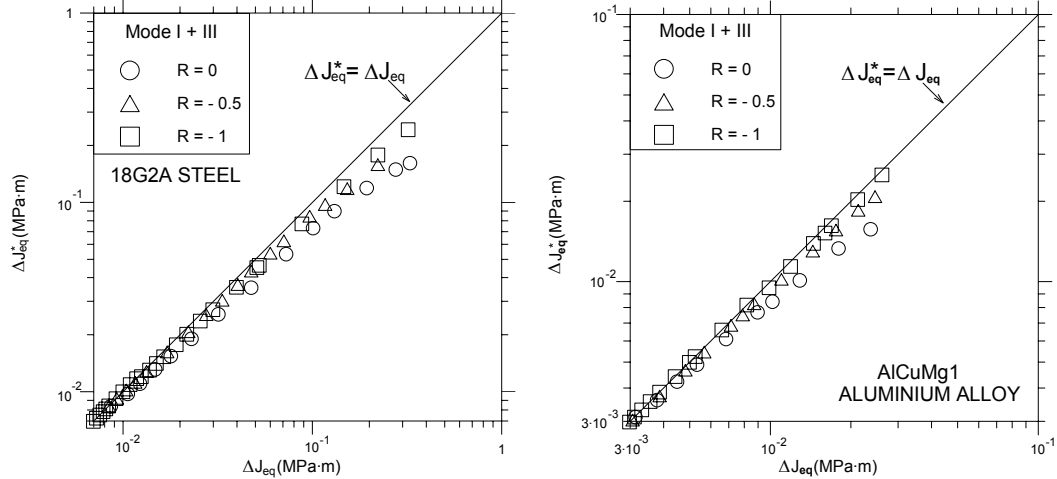


Figure 5: The relationship between ΔJ_{eq}^* and ΔJ_{eq} for a) 18G2A and b) AlCuMg1.

analysed the correlation between the parameters ΔK_{eq} and ΔJ_{eq} . The following relation was used

$$\Delta J_{\text{eq}}^* = \left(1 - \nu^2\right) \frac{\Delta K_{\text{eq}}^2}{E} \quad (6)$$

The range of the equivalent stress intensity factor ΔK_{eq} calculated from eqn (2) to (4). Figs. 5a and 5b show the relation between the parameters ΔJ_{eq}^* and ΔJ_{eq} for three stress ratios R . A good linear relation (in the double logarithmic system) between these two parameters in the case of the fatigue crack growth rate for the tested materials was observed. In 18G2A steel, this occurs for $\Delta J_{\text{eq}} <$

$1 \cdot 10^{-2}$ MP·m (Fig. 5a) and in AlCuMg1 aluminium alloy for $\Delta J_{eq} < 7 \cdot 10^{-3}$ MP·m (Fig. 5b). This means that in this test range under controlled loading, the parameter ΔJ_{eq} plays a similar role to the parameter ΔK_{eq} up to the moment when plastic strain occurs. When plastic strains increase, we can find an increasing difference between ΔJ_{eq}^* and ΔJ_{eq} . The difference results from the fact that the parameter ΔJ_{eq}^* does not include plastic strains. At the final stage of specimen life, when ΔJ_{eq} integral range approaches the critical value of J_{Ic} , the crack growth rate increases rapidly (Fig. 5a, $R = 0$) and leads to the material failure.

4 CONCLUSIONS

From the test results for fatigue crack growth in 18G2A steel and AlCuMg1 aluminium alloy under proportional cyclic bending with torsion, the following conclusions can be drawn:

1. The applied model (5) including ΔJ integral range is good for description of fatigue crack growth rate tests in mixed mode I + III.
2. It has been shown that the applied parameter ΔJ_{eq} as compared with the parameter ΔK_{eq} for different stress ratios R is better for description of crack growth rate in 18G2A steel and AlCuMg1 aluminium alloy.
3. It has been found that the mean value has got a very unfavourable effect on the crack growth rate in the aluminium alloy AlCuMg1 (it strongly decreases its life).

REFERENCES

- [1] Qian J. and Fatemi A., Mixed mode fatigue crack growth: a literature survey, Eng. Fracture Mechanics, vol.55, pp. 969-990, 1996.
- [2] Yates J.R., Fatigue thresholds under mixed-mode (I+III) loading, Int. J. Fatigue, vol.13, pp. 383-388, 1991.
- [3] Yates J.R. and Miller K.J., A torsion-bending loading frame for use with a uniaxial test machine, Fatigue Fract. Eng. Mater. Struct., vol.11, pp. 321-330, 1988.
- [4] Kimachi H., Tanaka K., Akiniwa Y. and Yu H., Elastic-plastic fatigue crack propagation under mixed mode of I and III loading, Sixth International Conference on Biaxial/Multiaxial Fatigue & Fracture, Lisboa, pp. 605-612, 2001.
- [5] ASTM E813 – 89, American Society for Testing and Materials, Philadelphia, 1987.
- [6] Macha E. and Rozumek D., Fatigue crack path development in a one-sided restrained bar with a rectangular section and stress concentrator under bending, International Conference on Fatigue Crack Paths, edited by A. Carpinteri, Parma, pp. 60 and CD-ROM, 8 ps, 2003.
- [7] Achtelik H. and Jamroz L., Patent PRL No.112497, CSR No.200236 and HDR No.136544, Warsaw, Poland, 1982.
- [8] Rozumek D., Influence of the mean loading on fatigue crack growth rate and life under bending, Journal of Theoretical and Applied Mechanics, vol. 42, pp. 83-93, 2004.

Acknowledgements: This work was supported by the Commission of the European Communities under the FP5, GROWTH Programme, contract No. G1MA-CT-2002-04058 (CESTI)